VERSITA

Arch. Min. Sci., Vol. 57 (2012), No 3, p. 497–515

Electronic version (in color) of this paper is available: http://mining.archives.pl

DOI 10.2478/v10267-012-0033-2

STANISŁAW WOLNY*

THE INFLUENCE OF OPERATING LOADS ON THE STATE OF STRESS AND STRAIN IN SELECTED LOAD-BEARING ELEMENTS OF A TOWER-TYPE HEADGEAR STRUCTURE

WPŁYW OBCIĄŻEŃ EKSPLOATACYJNYCH NA STAN NAPRĘŻENIA ORAZ PRZEMIESZCZENIA WYBRANYCH ELEMENTÓW NOŚNYCH KONSTRUKCJI BASZTOWEJ WIEŻY SZYBOWYCH

The headgear structure allows the conveyance to be moved over the shaft top to the loading (unloading) point, at the same time it keeps in place the rope pulleys while tower-type headgear structures also accommodate the entire winder installations.

The headgear is where the final stage of the hoisting installation is located and where the surface transport systems begin. These aspects strongly impact the actual shape of the tower, its height and in some cases determine the design of the entire winding gear.

In order that all the headgear functions should be provided, it is required that the ultimate state conditions should be maintained throughout its entire service life. In order to assess the critical service conditions, the computation procedure should be applied based on design loads and fatigue endurance parameters.

The computations of characteristic loads acting on the headgear structure use the developed model of the system based on the dynamic analysis carried out for a specific case: a hoisting installation operated in one of the underground collieries in Poland. The maximal and minimal loads acting on a Koepe pulley and those required for the system operation are determined accordingly.

The laws of dynamics provide a background for finding the forces and moments of forces acting in the components of the driving system (including the electric motors and pulley blocks) for the specified loading of the Koepe pulley.

Underlying the numerical FEM model of the tower-type headgear structure are the technical specifications of the analysed object and FEM calculations followed by endurance analysis to find the state of stress in structural elements of the headgear under the typical service conditions.

The results help in assessing how the design of the hoisting installation should impact on safety features of load-bearing elements in the headgear structure.

Keywords: tower-type headgear, state of stress, loading

Wieża szybowa jest konstrukcją umożliwiającą wyprowadzenie naczynia wydobywczego ponad zrąb szybu do miejsca wyładunku (bądź załadunku) i jednocześnie podtrzymuje koła linowe, a w przypadku wież basztowych, całą maszynę wyciągową.

* AGH UNIVERSITY OF SCIENCE AND TECHNOLOGY, FACULTY OF MECHANICAL ENGINEERING AND ROBOTICS, AL. MICKIEWICZA 30, 30-059 KRAKÓW, POLAND

W wieży mieści się końcowy odcinek transportu pionowego i zaczyna transport powierzchniowy. Fakt ten w istotny sposób wpływa na kształt wieży, w tym na jej wysokości, a często decyduje o konstrukcyjnym rozwiązaniu całego urządzenia wyciągowego.

W tym kontekście, poprawne spełnienie wszystkich funkcji wieży szybowej, będzie na etapie eksploatacji urządzenia, wymagać zapewnienia warunków stanu granicznego użytkowalności. Obliczenie stanu granicznego użytkowalności, wymagają stosowania obliczeniowych wartości obciążeń i obliczeniowych wartości wytrzymałości.

W celu wyznaczenia charakterystycznych wartości obciążeń konstrukcji wieży szybowej, w oparciu o opracowany model układu, przeprowadzoną analizę dynamiczną, przykładowo dla urządzenia wydobywczego pracującego w jednej z polskich kopalń, wyznaczono maksymalne i minimalne wartości obciążenia konstrukcji koła pędnego, konieczne do realizacji procesu.

Korzystając z zasad dynamiki, dla określonych wartości obciążenia koła pędnego, wyznaczono siły i momenty w elementach układu napędowego, w tym silników elektrycznych, kół kierujących.

Bazując na dokumentacji technicznej analizowanego obiektu, opracowano model numeryczny MES konstrukcji nośnej wieży szybowej, a następnie wykonano analizę wytrzymałościową – stanu naprężenia w elementach konstrukcyjnych wieży szybowej – wywołanego normalną eksploatacją wyciągu.

Wyniki przeprowadzonych analiz i obliczeń, pozwoliły na ocenę wpływu podstawowych parametrów wyciągu, na bezpieczeństwo eksploatacji elementów nośnych konstrukcji wieży szybowej.

Słowa kluczowe: basztowe wieże wyciągowe, stan naprężenia, obciążenia

1. Introduction

The headgear structure allows the conveyance to be moved over the shaft top to the loading (unloading) point, at the same time it keeps in place the rope pulleys whilst tower-type headgear structures also accommodate the entire winder installations.

The headgear is where the final stage of the hoisting installation is located and where the surface transport systems begin. These aspects strongly impact the actual shape of the tower, its height and in some cases determine the design of the entire winding gear.

In order that all the headgear functions should be provided, it is required that the ultimate state conditions should be maintained throughout its service life. In order to assess the critical service conditions, the computation procedure should be applied based on design loads and fatigue endurance parameters.

The computations of characteristic loads of the headgear structure using the developed model of the system are based on the dynamic analysis carried out for a specific case: a hoisting installation operated in a colliery in Poland (Wolny, 2009). The maximal and minimal loads acting on a Koepe pulley and those required for the system operation are determined accordingly (chapter 4).

The laws of dynamics provide a background for finding the forces and moments of forces acting in the components of the driving system (including the electric motors and pulley blocks) for the specified loading of the Koepe pulley (chapter 3).

Underlying the numerical FEM model of the tower-type headgear structure (chapter 4) are the technical specifications of the analysed object and FEM calculations followed by endurance analysis to find the state of stress in structural elements of the headgear under the typical service conditions (chapter 5).

The results help in assessing how the design of the hoisting installation should impact on safety features of load-bearing elements in the headgear structure.

2. Koepe pulley loading due to operation of the hoisting installation

Dynamic analyses (Wolny, 2009; Wolny, & Matachowski, 2010) and verification measurements taken on a real object (Wolny & Płachno, 2009) yield the maximal and minimal forces acting in hoisting ropes at the instant they slide onto and out of the Koepe pulley within one duty cycle of the hoisting gear.

Presented below are technical parameters of a hoisting gear operated in a colliery in Poland. Its headgear structure is the subject of the rigorous endurance analysis.

2.1. Technical parameters of the hoisting gear

The schematic diagram of the hoisting gear is shown in Fig. 1.

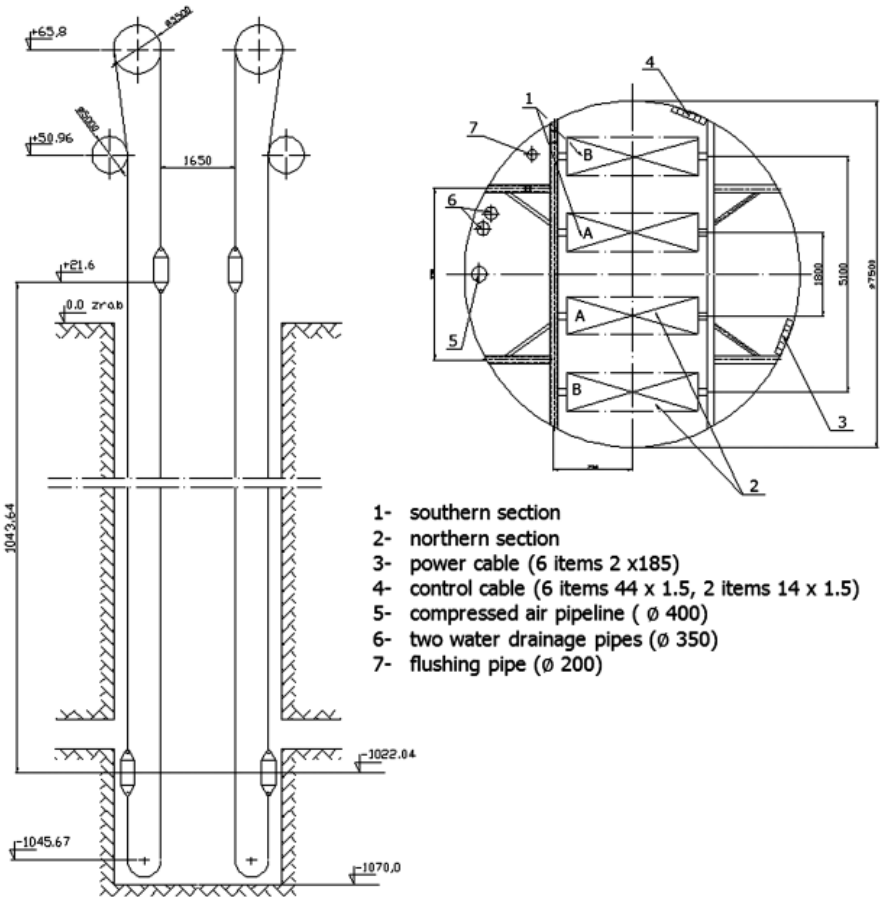

Fig. 1. Schematic diagram of the hoisting gear

Major technical parameters of the hoisting gear:
- winder type 4L-5500/2 × 3600,
- dc motor drive 2 × 3600 kW,
- nominal *rpm n* = 77 rpm,
- maximal skip velocity V = 20 m/s,
- skip mass with attachments m_{ku} =37800 kg,
- payload m_u = 30 000 kg

Mass moment of inertia GD^2:
- Koepe pulley GD_T^2 = 773000 kGm^2,
- Drive pulley GD_k^2 = 220000 kGm^2,
- Rotor 2 GD_{ws}^2 = 2 × 141000 kGm.

Reduced rotating mass g ≅ 10 m/s^2
Hoist ropes:

$$M_0 = \frac{1}{g} \cdot (G_{zrB} + G_{zrW} + G_{zrK}) = 1/10(25600 + 9340 + 8800) = 43740 \text{ kg}$$

- number n_{l_N} = 4,
- length l_N = 1130 m,
- diameter ϕ_N = 52 mm,
- total cross section area A_N = 1140 m^2,
- breaking force $S_z = 4 \cdot 2018 = 8072$ kN
- unit mass of 1 meter of a hoist rope q_N = 10,80 kg/mb.

Tail ropes
- number n_{l_w} = 4,
- length l_w = 1069,09 m,
- diameter ϕ_w = 55 mm,
- total cross-section area of wires A_w = 1195 m^2,
- unit mass of 1 meter of a tail rope q_w = 10,9 kg running/meter,

The function governing the Koepe pulley loading over the full duty cycle is derived, taking into account the key parameters of the hoisting gear:
- acceleration during the start-up phase a_1 = 1,0 m/s^2,
- deceleration in the braking phase a_2 = 1,2 m/s^2.

Elastic parameters of hoist ropes:
- Young's modulus E_N = 110 GPa,
- cross-section area of the set of hoist ropes $\sum A_N = 4 \cdot A_N = 4 \cdot 1140 = 4560$ m^2,
- velocity of elastic wave propagation in ropes a_N = 3700 m/s

2.2. Koepe pulley loading

The dynamic analysis of the hoist installation (Wolny, 2011) yields the maximal loading of the Koepe pulley in the typical duty cycle:

a) start-up phase – hoisting of a full conveyance from the bottom level with the acceleration a_1 (the maximal loading acting on the Koepe pulley)
b) braking phase – the full conveyance approaching the top level with the deceleration a_2 (minimal loading acting on the Koepe pulley).

2.2.1. Koepe pulley loading in the start-up phase – (a full conveyance is hoisted with the acceleration a_1)

A. Ropes on the end of the hoisted conveyance

a) Maximal dynamic overloading in the hoisting rope at the point the rope passes onto the pulley is given as (Wolny, 2011):

$$\Delta S^R = A_N E_N \frac{a_1}{a_N} \frac{8 l_N}{a_N} \left[1 - e^{-k}\right] \cdot \frac{1}{k} \tag{1}$$

In the start-up phase:

$A_N = 4560 \cdot 10^{-6}$ m^2 — totalled cross-section area of hoisting ropes,
$E_N = 110$ GPa — modulus of elasticity of hoisting ropes,
$a_1 = 1{,}0$ m/s^2 — acceleration in the start-up phase,
$a_N = 3700$ m/s — velocity of elastic wave propagation in hoisting ropes,
$l_N = 1087{,}84$ m — length of hoisting ropes (from the conveyance attachment to the Koepe pulley at the instant the conveyance begins to be hoisted with acceleration a_1)

$$k = h_2 \frac{2 I_N}{a_N}, \quad h_2 = \frac{A_N E_N}{M_2 a}$$

$M_2 = m_u + m_{ku} = 33000 + 37800 = 70800$ kg – mass of the conveyance plus the payload.
Substituting these values in Eq (1) we get:

$$\Delta S^R = 117{,}2 \text{ kN}.$$

b) Koepe pulley loading due to the mass of the conveyance and the payload

$$G_1 = M_2 \cdot 9{,}81 \text{ kg} \frac{\text{m}}{\text{s}^2}$$

where:
$M_2 = m_u + m_{ku} = 33000 + 37800 = 70800$ kg – mass of the conveyance plus the payload
Hence

$$G_1 = 70800 \cdot 9{,}81 = 694{,}5 \text{ kN}$$

c) Koepe pulley loading due to the weight of hoisting ropes

$$G_{l_N} = 4 \cdot q_N \cdot l_N \cdot 9{,}81$$

where:
$q_N = 10{,}8$ kg/mb – mass of one running meter of hoist ropes,
$l_N = 1087{,}84$ m – length of hoist ropes,
Hence

$$G_{l_N} = 4 \cdot 10{,}8 \cdot 1087{,}84 \cdot 9{,}81 \cong 461{,}0 \text{ kN}.$$

The overall loading of the Koepe pulley on the end of the hoisted conveyance at the point where hoist ropes slide onto the pulley (static and dynamic load).

$$S_1 = \Delta S^R + G_1 + G_{l_N} = 117{,}2 + 694{,}5 + 443{,}5 \cong 1272{,}7 \text{ kN}$$

B. Ropes on the side of the conveyance being lowered
a) Koepe pulley loading due to the weight of an (empty) conveyance

$$G_2 = m_{ku} \cdot 9{,}81 \text{ kg}\frac{\text{m}}{\text{s}^2},$$

where:
$m_{ku} = 37800$ kg – mass of the conveyance
Hence:

$$G_2 = 37800 \cdot 9{,}81 = 370{,}818 \text{ kN}$$

b) Koepe pulley loading due to the weight of hoisting ropes

$$G^*_{l_N} = 4 \cdot q_N \cdot l^*_N \cdot 9{,}81 \ \frac{\text{kg}}{\text{m}}\text{m}\frac{\text{m}}{\text{s}^2},$$

where:
$l^*_N = 44{,}2$ m – hoisting rope length on the side of the conveyance being lowered,
$q_N = 10{,}80$ kg/mb – mass of a running meter of a hoisting rope
Hence

$$G^*_{l_N} = 4 \cdot 10{,}80 \cdot 44{,}2 \cdot 9{,}81 = 18{,}73 \text{ kN}$$

c) Koepe pulley loading due to the weight of tail ropes

$$G^*_{l_N} = 4 \cdot q_{w_1} \cdot l^*_w \cdot 9{,}81$$

where:
$q_{w_1} = 10{,}9$ kg/mb
$l^*_w = 1000{,}2$ m – length of tail ropes (from the tail rope attachment to the return point in the shaft sump).

Hence

$$G^*_{l_w} = 4 \cdot 10{,}9 \cdot 1000{,}2 \cdot 9{,}81 = 427{,}8 \text{ kN}$$

Koepe pulley loading on the side of the conveyance being lowered, at the point where hoisting ropes slide off the pulley

$$S_2 = G_2 + G^*_{l_N} + G^*_{l_w} = 370{,}818 + 18{,}73 + 427{,}8 \cong 817{,}35 \text{ kN}$$

C. Rotating mass in the headgear reduced on the rope axis

$$M_0 = 43740 \text{ kg},$$

D. d'Alambert's dynamic equation (an equilibrium condition, see Fig. 2)

$$P_0 = S_1 + M_0 \cdot a - S_2 = 1272{,}7 + 43{,}740 \cdot 1{,}0 - 817{,}34 \cong 499 \text{ kN}$$

where:
P_0 – circumferential force,
$a_2 = 1{,}0$ m/s^2 – acceleration in hoisting,
Hence the torque becomes:

$$M_{ob} = P_0 \cdot r = 499 \cdot 2{,}750 = 1372{,}25 \text{ kNm}$$

where: $r = 2750$ mm – mantle radius in the Koepe pulley

The Koepe pulley loading in this case is shown in Fig. 2.

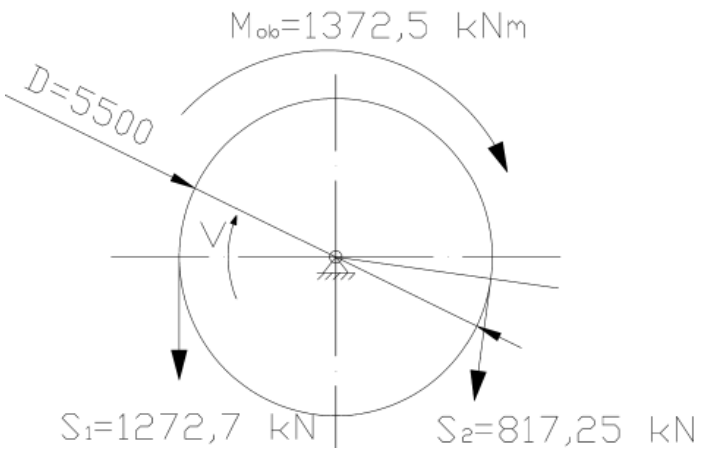

Fig. 2. Koepe pulley loading while the conveyance is being hoisted

2.2.2. Koepe pulley loading at the instant the braking phase begins (when the full conveyance reaches the top level)

A. Ropes on the end of the braking conveyance

a) The maximal loading acting on the hoisting ropes at the point they slide onto the pulley (Wolny, 2011).

$$\Delta S^{H}_{l_{N\max}} = -A_N E_N \frac{a_2}{a_N} \frac{20{,}5 l^*_N}{a_N} \tag{2}$$

where:

$l^*_N = 250$ m – hoisting rope length (from the full conveyance to the Koepe pulley at the instant the braking phase begins)

$a_2 = 1{,}2$ m/s^2 – deceleration when braking,

The remaining parameters are identical as in 2.2.1.

Substituting the numerical values to Eq (2) yields:

$$\Delta S^{H}_{l_{N\max}} = -4560 \cdot 10^{-6} \cdot 1{,}1 \cdot 10^{11} \frac{1{,}2}{3700} \cdot \frac{250}{3700} = -225 \text{ kN}$$

b) Koepe pulley loading due to the weight of the conveyance and payload

$$G_1 = M_2 \cdot 9{,}81 = 694{,}5 \text{ kN}$$

c) Koepe pulley loading due to the weight of hoisting ropes

$$G^*_{l_N} = 4 \cdot q_N \cdot l^*_N \cdot 9{,}81 = 4 \cdot 10{,}80 \cdot 250 \cdot 9{,}81 \cong 106 \text{ kN}$$

d) Koepe pulley loading due to tail ropes

$$G_{l_w} = 4 \cdot q_w \cdot l_w \cdot 9{,}81 = 4 \cdot 10{,}9 \cdot 961{,}47 \cdot 9{,}81 \cong 368{,}5 \text{ kN}$$

The actual loading of the Koepe pulley on the side of the conveyance approaching the top station (static + dynamic load)

$$S^*_1 = G_1 + G_{l^*_N} + G_{l_w} - \Delta S^{H}_{l_{N\max}} = 694{,}5 + 106 + 368{,}5 - 225 \cong 944 \text{ kN}$$

B. Ropes on the side of the (empty) conveyance being lowered

a) Koepe pulley loading due to the conveyance weight

$$G_2 = m_{ku} \cdot 9{,}81 = 37800 \cdot 371{,}0 \text{ kN}$$

b) Koepe pulley loading due to the weight of hoisting ropes

$$G_{l^*_N} = 4 \cdot q_N \cdot l^*_N \cdot 9{,}81 = 4 \cdot 10{,}8 \cdot 837{,}8 \cdot 9{,}81 = 355{,}1 \text{ kN}$$

c) Koepe pulley loading due to the weight of tail ropes

$$G_{l_w^*} = 4 \cdot q_w \cdot l_N^* \cdot 9{,}81 = 4 \cdot 10{,}9 \cdot 272 \cdot 9{,}81 = 116{,}34 \text{ kN}$$

The total Koepe pulley loading on the side of the conveyance being lowered at the point hoisting ropes slide off the pulley

$$S_2^* = G_2 + G_{l_N^*} + G_{l_w^*} = 371{,}0 + 355{,}1 + 116{,}34 = 842{,}44 \text{ kN}$$

C. Rotating mass in the headgear reduced on the rope axis,

$$M_0 = 43740 \text{ kg}$$

D. d'Alambert's dynamic equation

$$P_0 = S_1^* - M_0 a_2 - S_2^* = 994 - 43{,}73 \cdot 1{,}2 - 842{,}44 \cong 99{,}08 \text{ kN}$$

where:
P_0 – circumferential force,
a_2 – deceleration whilst in braking.

Hence the moment of circumferential force becomes:

$$M_{ob} = P_0 \cdot r = 99{,}08 \cdot \frac{5{,}5}{2} = 272 \text{ kN}$$

where: $r = \frac{5{,}5}{2}$ m – drum radius

This case of Koepe pulley loading is shown in Fig. 3.

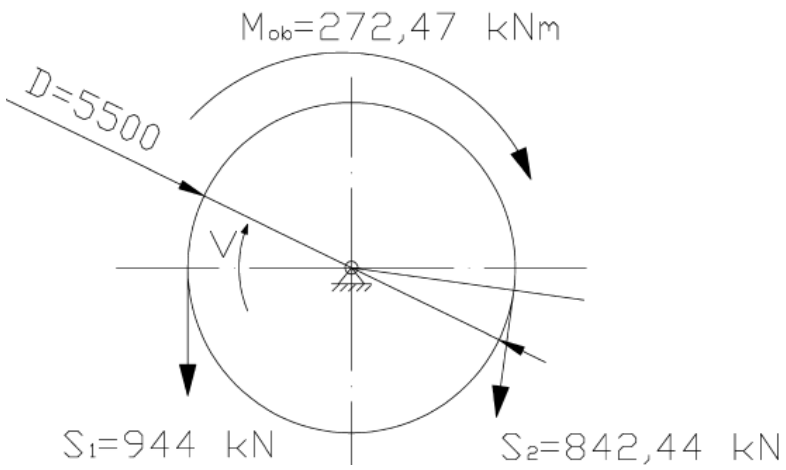

Fig. 3. Koepe pulley loading at the instant the full conveyance begins to brake when approaching the bottom level

3. Loading of the tower-type headgear structure due to hoist operation

The model of the tower-type headgear structure in the hoisting installation shown in Fig. 4 incorporates the driving system elements that carry the loads due the payload being hauled onto the headgear structure:

- drum with the rope winding diameter D_B = 5500 mm supported at the point where elements are mounted in bearings (1)
- driving pulleys with the rope winding diameter D_B = 5000 mm supported at the point where elements are mounted in bearings (2)
- two dc motors PW-106 with the power ratings N = 3600 KW generating the driving moment (3)

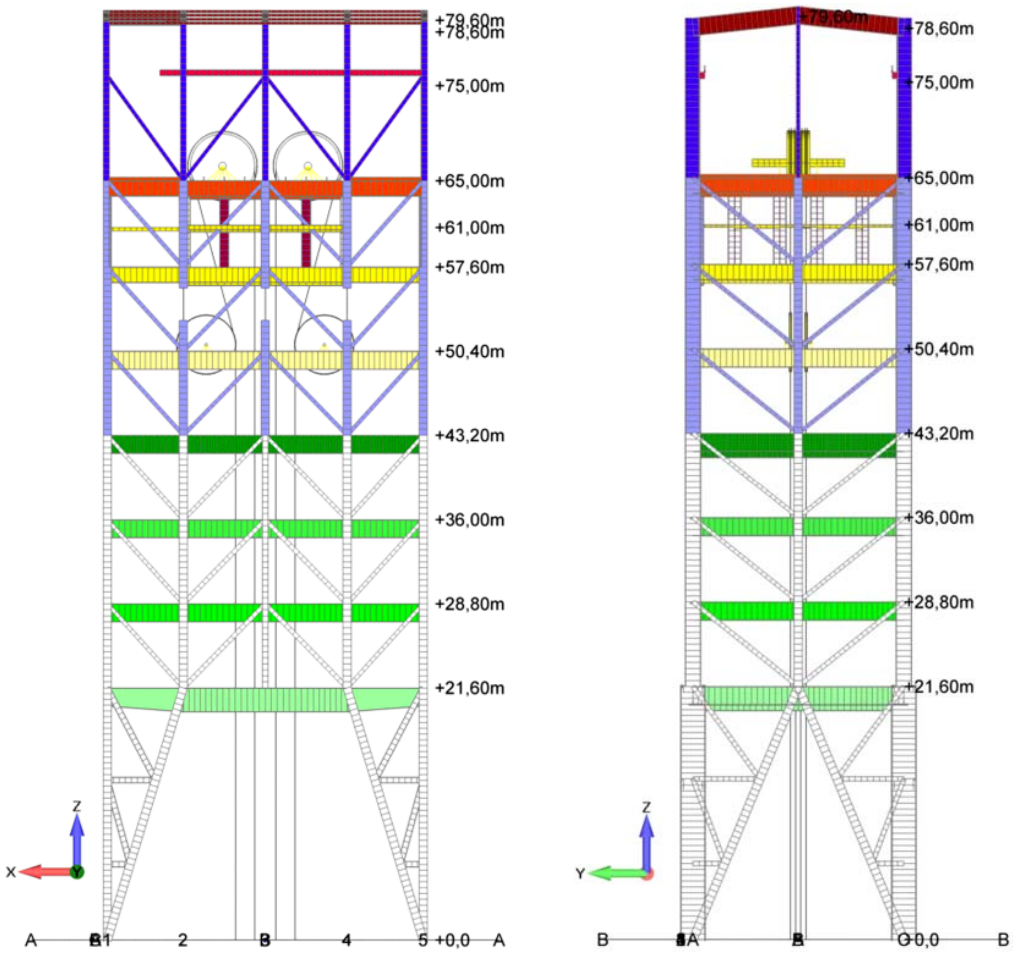

Fig. 4. Tower-type headgear model showing the driving system components

Under the typical operating conditions the headgear loading involves the forces generated in the driving system elements whilst the payload in the skip is hoisted upwards and lowered. The loads applied to the bearing elements in the headgear structure for two extreme cases of the Koepe pulley and driving pulley loading (minimal and maximal loading), shown schematically in Fig. 5, are obtained from the dynamic analysis of the hoisting installation (Wolny, 2011):

a. minimal loads- when the full conveyance begins to brake when approaching the top level (Fig. 5)
b. maximal loads- when the full conveyance is being hoisted upwards from the bottom level (Fig. 5)

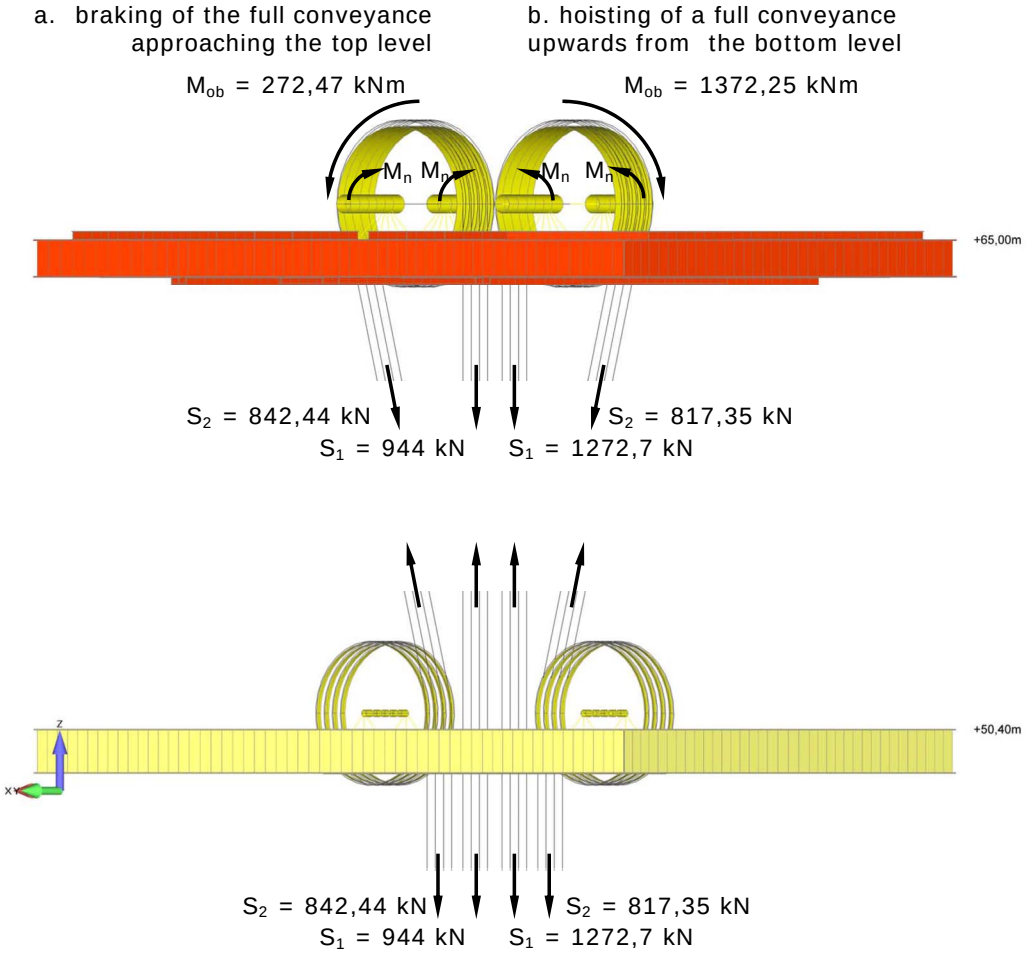

Fig. 5. Loads acting upon driving elements mounted in the headgear structure (Koepe pulley and rope pulleys)

4. FEM model of the tower-type headgear

Technical documentation of the object provides the backgrounds for the numerical model of the load-bearing structure of the headgear tower, shown in Fig. 6.

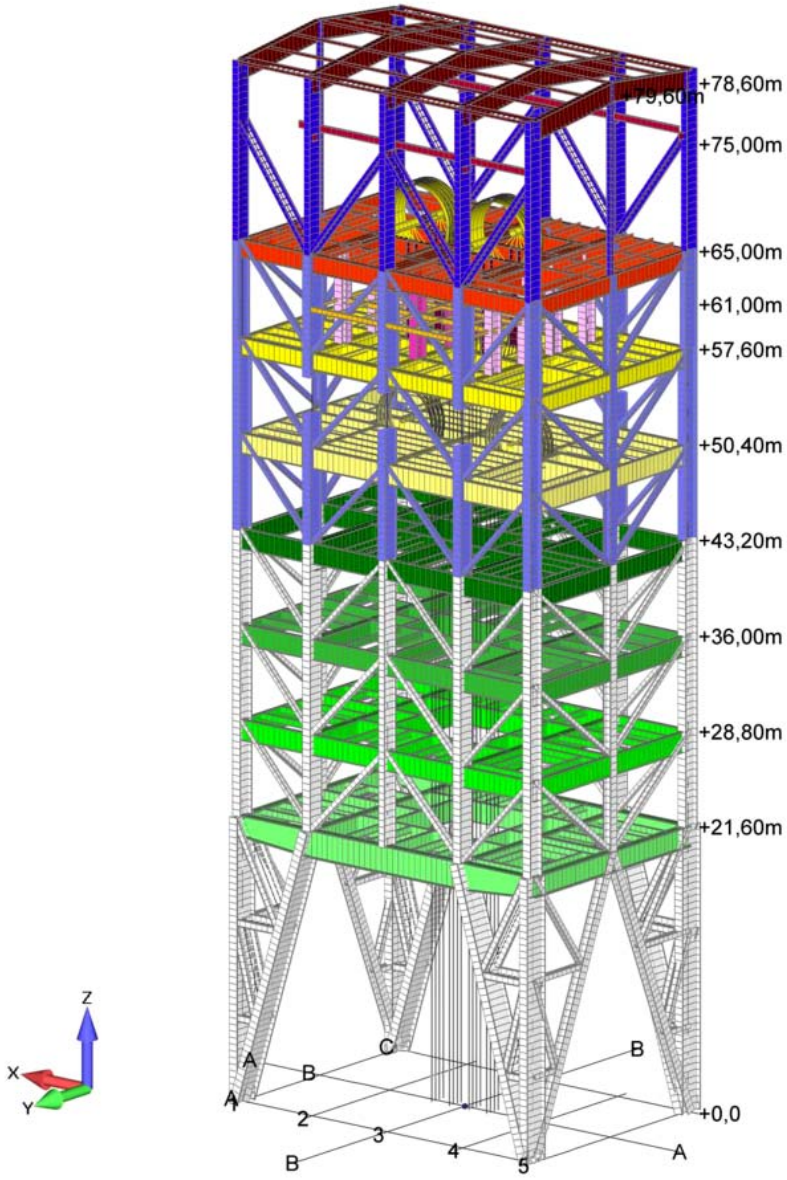

Fig. 6. Numerical model of the load-bearing structure of the headgear

The developed numerical model of the load-bearing structure of the headgear is the beam-surface model, incorporating the following elements:

- trestles and transoms of a frame
- transverse and longitudinal beams acting as the plating on stage levels
- bracing in longitudinal sections and cross sections at stage levels

The feet of trestles making up the exterior frame are stabilised in foundations. On the level (+65.00 m) the driving elements are fixed (modelled), including the Koepe pulley with the rotors and stators of the electric motor and on the level (+50.4 m) is the driving pulley. The elements of the driving system are subjected to forces whose values are obtained from the dynamic analysis (Wolny, 2011) and from the calculation procedure outlined in chapter 2 and 3. The systems of forces applied to the driving elements and the structural components are shown schematically in Fig. 5.

5. Results of endurance analysis using the FEM approach

The endurance analysis of the state of stress and strain in structural elements of a tower-type headgear structure is performed for two extreme cases: the minimal and maximal loading conditions (chapter 3,4).

The numerical data (i.e. the states of stress in structural elements of the tower type headgear) are shown graphically in Figs 7-10.

Based on the von Mises hypothesis, the reduced stress distribution σ_z is derived in load-nearing elements of the headgear from the level +57.60 m to +75.00 (Fig. 7). The largest reduced stress is registered in load-bearing roof beams +65.00, near the winding gear. In order that the state of stress in the beams at the level +65.00 should be precisely determined, this fragment of the headgear structure is shown in Fig. 8, with indicated stress contour lines.

The largest values of reduced stress (about 20 MPa) are registered at connection points of beams supporting the shaft bearing and the stator. The stress concentration points in these areas are shown in Fig. 9.

Results of endurance analysis shown in Figs 7-10 reveal the maximal loads experienced by the driving element in the hoisting gear when the full conveyance begins to be hoisted from the bottom level, with the acceleration a_1.

Results of numerical analysis of the state of stress in structural elements of the headgear under the load acting when the full conveyance begins to brake when approaching the top level are shown in Fig 10. The numerical data are restricted to the distribution of reduced stress σ_z derived based on the Huber-von Mises hypothesis in load-bearing elements of the headgear structure at the levels from +57.60 m to +75.00. The highest levels of reduced stress (around 13 MPa) are registered in beams at the level +65, near the winder installation, as in the case of the full conveyance beginning to move upwards from the bottom station.

The numerical analysis of displacements is restricted to compilation of displacements of rotors' axes with respect to the stators' axes in dc motors (these components being fixed separately). Displacements of the rotor's axis with respect to the stator's axis are shown schematically in Fig 11. The remaining displacement data are summarised in Table 1.

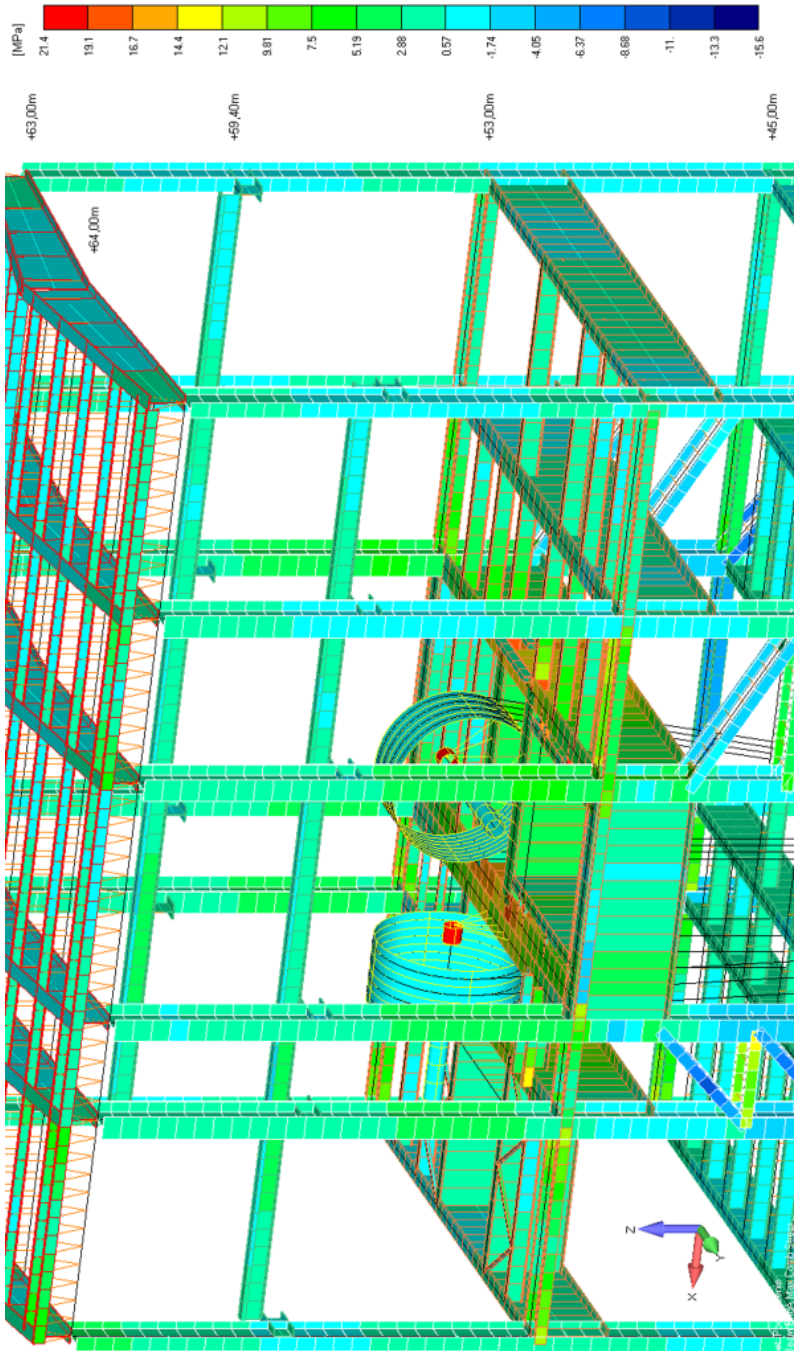

Fig. 7. Reduced stress distribution σ_z in load-bearing elements of the headgear structure at the levels from +57.60 m to +75.00 at the instant the full conveyance begins to be hoisted from the bottom level, with the acceleration a_1

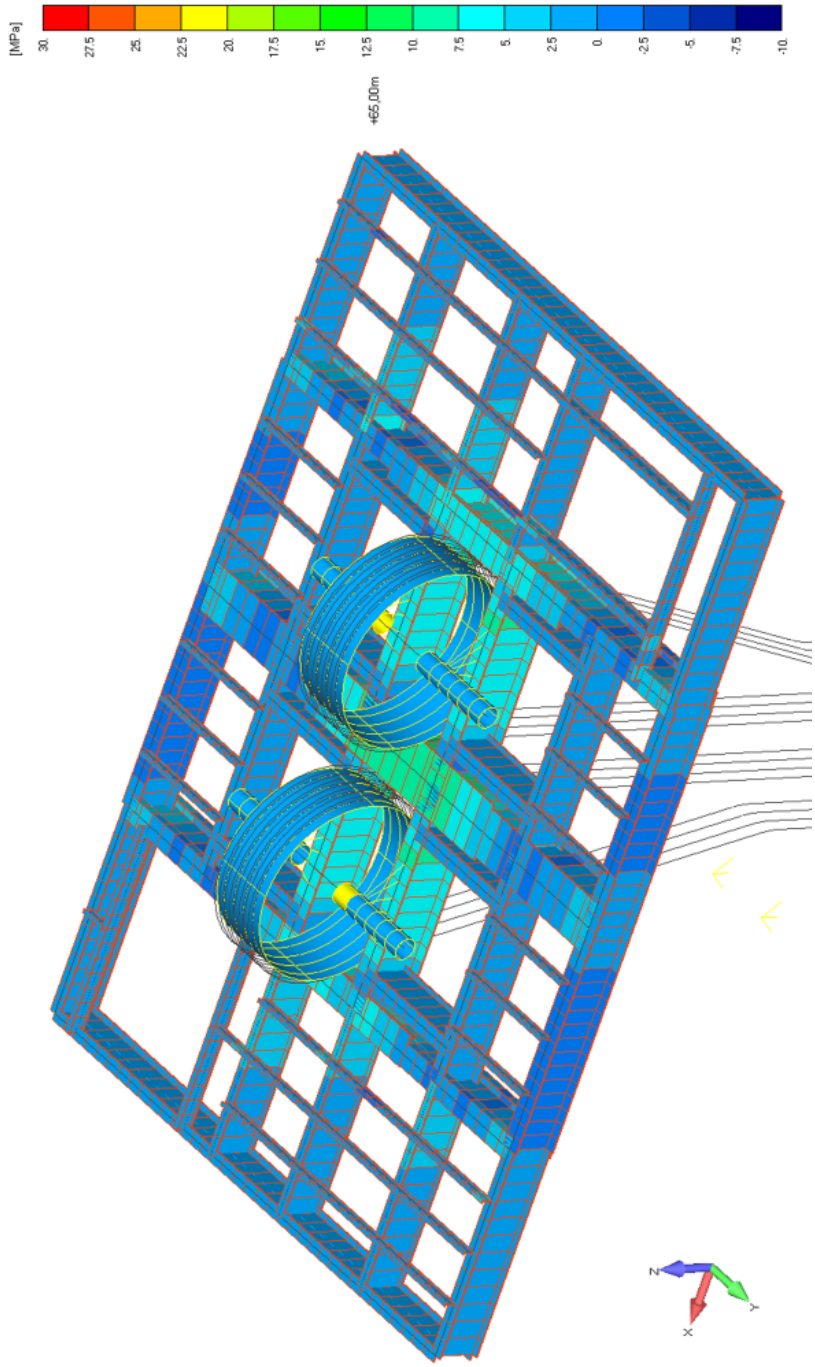

Fig. 8. Reduced stress distribution σ_z in beams at the level +65.00 (the view of the load-bearing structure) at the instant the full conveyance begins to be hoisted from the bottom level, with the acceleration a_1

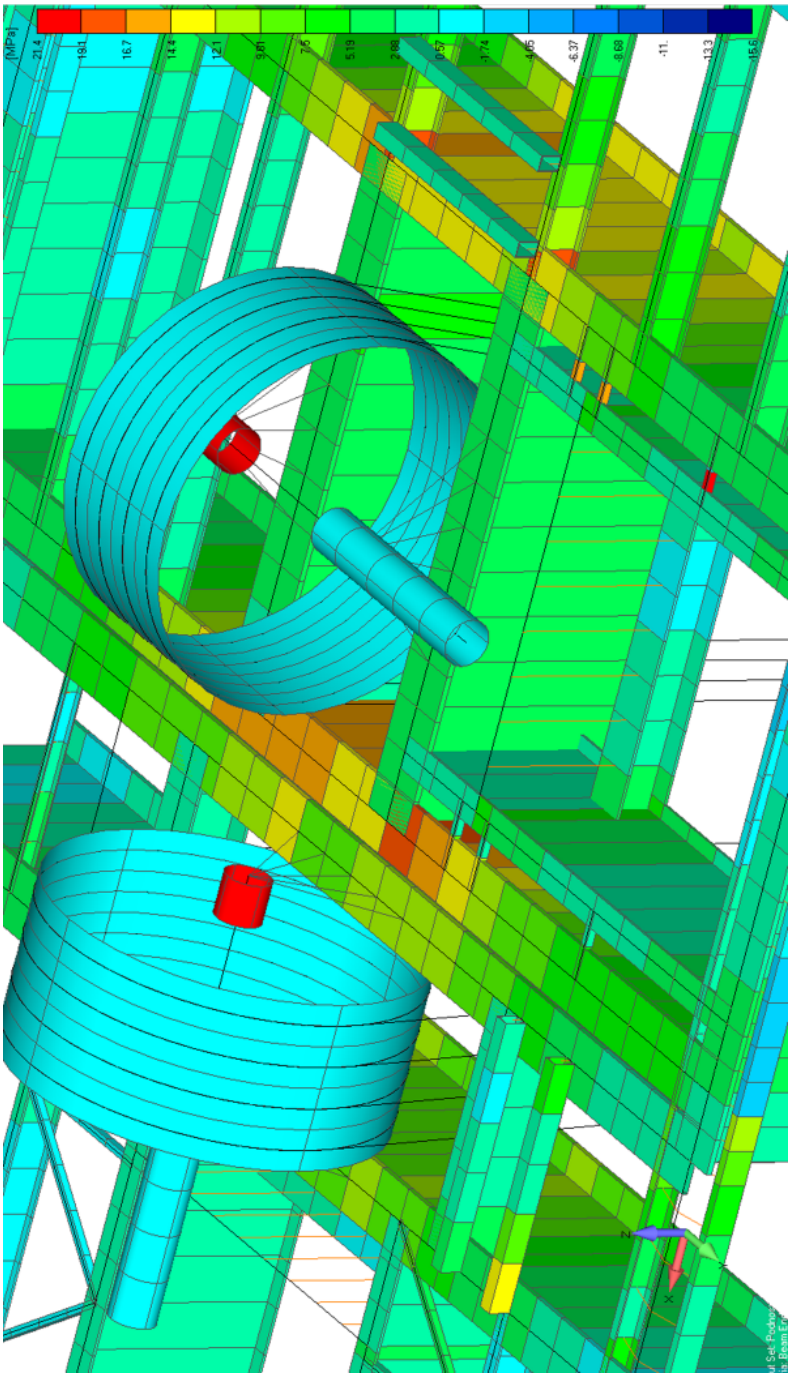

Fig. 9. Stress concentration in beams at the level +65.00 m, near the winding gear when the full conveyance begins to be hoisted from the bottom level, with the acceleration a_1

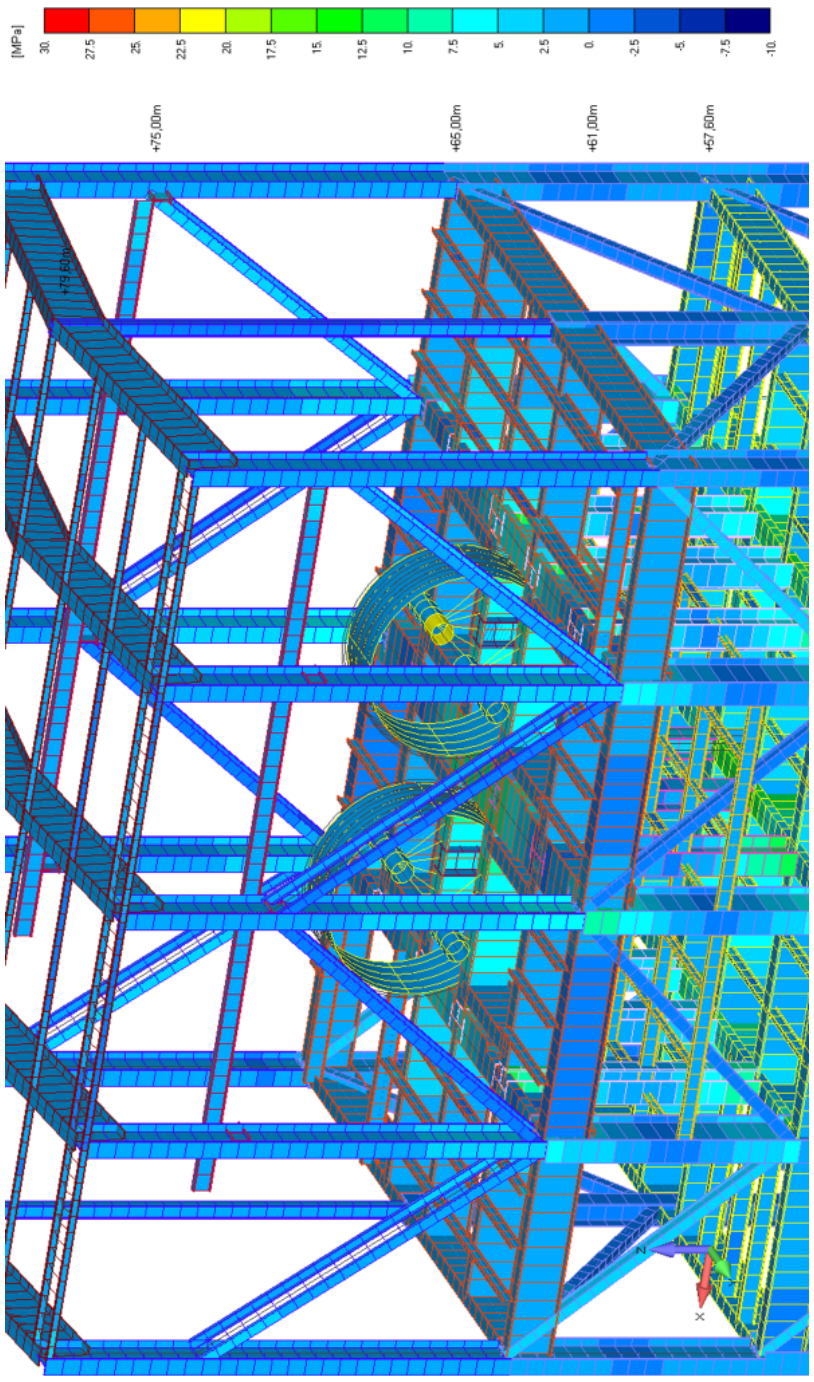

Fig. 10. Reduced stress distribution σ_z in load-bearing elements of the headgear structure at the levels from +57.60 m to +75.00 when the full conveyance begins to brake when approaching the top level

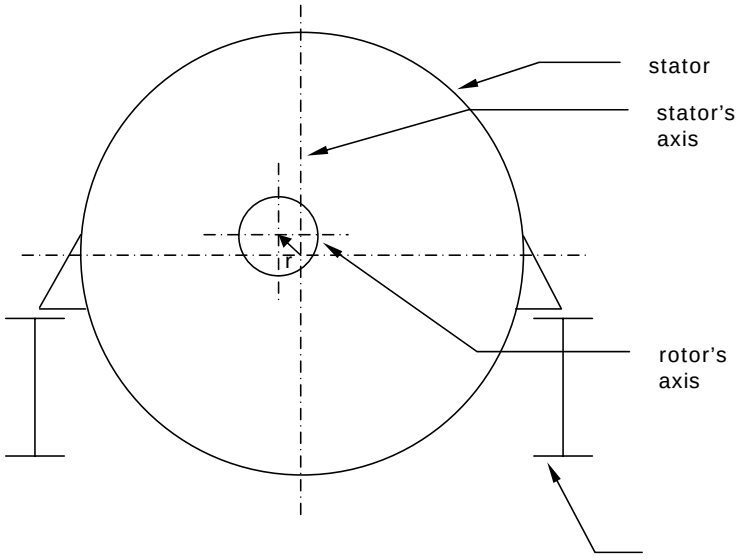

Fig. 11. Displacement of the rotor's axis with respect to that of the stator

TABLE 1

Displacement of the rotor's axis with respect to the stator's axis

Loading condition	**(Radial) displacement of the rotor's axis with respect to the stator's axis**
Hoisting of a full conveyance from the bottom level with the acceleration a_1	± 0.5 mm
Braking of a full conveyance approaching the top station with the deceleration a_2	± 0.4 mm

6. Summing-up

The endurance analysis allows for assessing the state of stress in load – bearing elements of the headgear structure and in connecting joints, taking into account the operational loads and variations of loading in time.

The maximal stresses in load-bearing elements of the headgear approach the level σ_z at points where the stators are fixed to the headgear's load-bearing structure, at the instant the full conveyance is hoisted upwards from the bottom station with the acceleration a_1, whilst the stress variation amplitude $\Delta\sigma$ should not exceed 10 MPa. The displacement vector follows a similar variability pattern, for example that representing the rotors' axes displacement with respect to the motor stators' axes under the extreme loading conditions: the maximal and minimal loads experienced throughout the typical duty cycle should not exceed 0.5 mm.

Results of endurance analyses and investigations of stress distribution and displacement vectors in the nodes and components of the load-bearing structure in a tower-type headgear fail

to provide sufficient backgrounds for the development of a reliable method of headgear control in the context of the usability criteria stipulated by the ultimate state method (PN-90/B-03200), due to relatively small values of relevant quantities (for example the maximal stresses σ with respect to the yield point Re of the manufacturing materials).

To improve reliability, theoretical data will be validated through measurements taken on a real object. Measurements will be performed to assess the state of stress in selected load-bearing elements and selected node strains in the headgear structure.

References

Wolny S., 2009. *Dynamic loading of the pulley block in a hosting installation in normal operating*. Arch. Min. Sci., Vol. 54, No 2, p. 261-284.

Wolny S., Płachno M., 2009. *Experimental verification of Bering rope loading in typical operating conditions of the hoisting installation*. Arch. Min. Sci., Vol. 54, No 3, p. 531-542.

Wolny S., Matachowski F., 2010.*Operating loads of the shaft steelwork – conveyance system due to random irregularities of the guiding strings*. Arch. Min. Sci., Vol. 55, No 3, p. 589-603.

Wolny S. i in., 2010. *Opracowanie metody kontroli fundamentów maszyn wyciągowych zainstalowanych na wieżach basztowych*. Praca naukowo-badawcza. Katedra Wytrzymałości, Zmęczenia Materiałów i Konstrukcji: AGH. Kraków (praca niepublikowana).

Wolny S., 2011. *Dynamic Loading of Conveyances in Normal Operating Conditions*. Arch. Min. Sci., Vol. 56, No 4, p. 665-685.

PN-90/B-03200; *Konstrukcje stalowe, obliczenia statyczne i projektowe.*

Received: 08 February 2012